Path-integral Monte Carlo calculation of the kinetic energy of condensed lithium

Claudia Filippi
Department of Physics, University of Illinois at Urbana-Champaign, Urbana, Illinois 61801

David M. Ceperley
National Center for Supercomputing Applications, University of Illinois at Urbana-Champaign, Urbana, Illinois 61801

(Received 23 May 1997)

We report path-integral Monte Carlo calculations of the kinetic energy of condensed lithium for several temperatures in both the solid and liquid phases. The excess kinetic energy of lithium decreases from about 10.4% of the classical value at 300 K to 3.2% at 520 K indicating a very slow decay with temperature. A Wigner-Kirkwood perturbation treatment of quantum effects to order $\hbar^2$ gives a satisfactory agreement with the path-integral results. [S0163-1829(98)06201-8]

I. INTRODUCTION

The momentum distribution of atoms in condensed matter can be directly measured by neutron Compton scattering. It has been determined for a variety of systems, including quantum solids and liquids formed from ^{3}He and ^{4}He (Ref. 1) and condensed noble gases,[2–5] in particular, neon. Most of the early work has been confined to liquid helium for its fundamental importance in connection to the theory of Bose condensation and Fermi liquids and because, due to the light mass and weak interactions, it is possible to probe its momentum distribution by thermal neutrons. With epithermal neutrons, the momentum distribution can now be determined for a larger number of materials. Recently, atomic Compton profiles of condensed Li, Be, B, C, and Al have also been measured.[6]

The momentum distribution for a classical system is of the Maxwell-Boltzmann form, an isotropic Gaussian $n(\mathbf{p}) = (3/2\pi)^{3/2} p_0^{-3} \exp\{-\frac{3}{2}(p/p_0)^2\}$ with $\hbar p_0 = (3mk_BT)^{1/2}$ where m is the atomic mass and k_B Boltzmann's constant. Quantum effects can give deviations from the Gaussian form. The momentum distribution shows distinct features for a system in the classical regime, an anharmonic crystal, a superfluid, or a Fermi liquid.

Condensed helium can show significant quantum behavior even up to room temperature, particularly at high pressures.[7,8] The transition to a classical behavior progressing through the noble gasses has been studied by neutron Compton scattering[3–5] and path-integral Monte Carlo (PIMC) calculations[2,5] by analyzing the second moment of the momentum distribution, the kinetic energy $\mathcal{K}$. Lithium is the next obvious candidate. It has been recently investigated by neutron Compton scattering up to room temperature[9] and experiments at higher temperatures are now in progress.[10] There are several theoretical studies of lithium near the melting point within classical molecular dynamics[11–15] and recent experimental investigation through neutron inelastic scattering[16] and high-resolution x-ray deep inelastic scattering.[17] Lithium is representative of the class of simple metals[18] and is a good test case for different theoretical approaches to liquid-state dynamics.[15]

Quantum effects in a system as light as lithium are certainly expected but, so far, they have not been quantified in a rigorous manner. Most of the theoretical and experimental investigations are near the melting temperature, $T_m = 453$ K, where the thermal wavelength $\Lambda = (2\pi\hbar^2/mk_BT)^{1/2}$ is significantly smaller than the average interparticle distance. Theoretical approaches rely on classical simulations and the quantum effects are believed to be properly accounted for in a simple perturbative approach in powers of $\hbar$.[19]

Since the kinetic energy gives a clear signature of the classical-quantum nature of a system, we performed PIMC calculations of the kinetic energy of ^{7}Li modeled as a collection of atoms interacting through a pairwise potential. We spanned a range of temperature around the melting point from $T = 300$ K to $T = 520$ K. The excess kinetic energy, defined as the difference of the kinetic energy, $\mathcal{K}$, and the classical value, $\mathcal{K}_{cl} = 3/2T$, decreases from 10.42% of the classical value at 300 K to 3.19% at 520 K. Therefore, the kinetic energy still differs from its classical value at temperature as high as 520 K confirming the slow decaying of the excess kinetic energy with temperature.[8] An inclusion of the leading quantum effects through an expansion of the kinetic energy in powers of $\hbar$ gives a satisfactory agreement with the PIMC results.

In Sec. II, we give a brief outline of the PIMC method. In Sec. III, we describe the interatomic potential chosen in our calculations. In Sec. IV, we present our results and a comparison with the values obtained from a perturbative treatment of quantum effects.

II. METHOD

The path-integral Monte Carlo method has been described in detail elsewhere.[20] Therefore, we will only give a brief outline of the method and present the aspects specific to the present calculation.

Let us consider a system of N particles described by a Hamiltonian $\mathcal{H}$. If the system is in thermodynamic equilibrium at a temperature T, the thermodynamic average of a physical observable $\mathcal{O}$ can be expressed as

$$\langle \mathcal{O} \rangle = \frac{\int d\mathbf{R} \langle \mathbf{R} | \mathcal{O} e^{-\beta\mathcal{H}} | \mathbf{R} \rangle}{\int d\mathbf{R} \langle \mathbf{R} | e^{-\beta\mathcal{H}} | \mathbf{R} \rangle}, \quad (1)$$

where $k_B T = 1/\beta$ and the configuration $\mathbf{R}$ indicates the positions of the N particles. If the density matrix is factorized as $e^{-\beta\mathcal{H}} = [\exp(-\tau\mathcal{H})]^M$ with a time step $\tau = \beta/M$, the expectation value [Eq. (1)] can be rewritten as

$$\langle \mathcal{O} \rangle = \frac{\int d\mathbf{R}\, d\mathbf{R}_1 \cdots d\mathbf{R}_{M-1} \langle \mathbf{R}| \mathcal{O} e^{-\tau\mathcal{H}} |\mathbf{R}_1\rangle \rho(\mathbf{R}_1,\mathbf{R}_2,\tau)\cdots\rho(\mathbf{R}_{M-1},\mathbf{R},\tau)}{\int d\mathbf{R}\, d\mathbf{R}_1 \cdots d\mathbf{R}_{M-1} \rho(\mathbf{R},\mathbf{R}_1,\tau)\rho(\mathbf{R}_1,\mathbf{R}_2,\tau)\cdots\rho(\mathbf{R}_{M-1},\mathbf{R},\tau)}, \tag{2}$$

where we adopted a position-space representation of the density matrix:

$$\rho(\mathbf{R},\mathbf{R}',\tau) = \langle \mathbf{R}| e^{-\tau\mathcal{H}} |\mathbf{R}'\rangle. \tag{3}$$

The evaluation of the integral [Eq. (2)] is performed by a generalization of the Metropolis Monte Carlo method: paths starting from different configurations $\{\mathbf{R}\}$ are sampled according to a probability distribution proportional to the product $\rho(\mathbf{R},\mathbf{R}_1,\tau)\rho(\mathbf{R}_1,\mathbf{R}_2,\tau)\cdots\rho(\mathbf{R}_{M-1},\mathbf{R},\tau)$ (if we ignore effects of quantum statistics). A path originates and terminates at the same configuration after $M-1$ steps. The quantity $\langle\mathcal{O}\rangle$ is obtained as the average over the paths of the ratio $\langle \mathbf{R}|\mathcal{O}e^{-\tau\mathcal{H}}|\mathbf{R}_1\rangle/\rho(\mathbf{R},\mathbf{R}_1,\tau)$.

For small enough time step τ (larger temperature), it is possible to obtain a sufficiently accurate approximation for the density matrix. However, for the calculation to be efficient, it is desirable to minimize the number M of slices. A good compromise between accuracy and number of slices is achieved by using the pair density matrix,

$$\rho(\mathbf{R},\mathbf{R}',\tau) \approx \rho^0(\mathbf{R},\mathbf{R}',\tau) \prod_{i<j} \exp[-u(r_{ij},r'_{ij},\tau)], \tag{4}$$

where $\rho^0(\mathbf{R},\mathbf{R}',\tau)$ is the free-particle density matrix and $u(r_{ij},r'_{ij},\tau)$ is defined to be exact for a pair of particles. r_{ij} and r'_{ij} are the distances between particles i and j in the configurations $\mathbf{R}$ and $\mathbf{R}'$, respectively. This density matrix is much more accurate than the commonly used primitive approximation, $u(r_{ij},r'_{ij},\tau) = \tau/2[V(r_{ij}) + V(r'_{ij})]$, where $V(r)$ is the interparticle potential. The effect of particle statistics can be included in the density matrix but, for our system at the temperatures of interest, such an effect is negligible and is not considered here.

In addition to the use of an accurate density matrix [Eq. (4)], we also use the virial estimator for the kinetic energy whose variance is four orders of magnitude smaller than the variance of the thermodynamic estimator, yielding a fast convergence of the calculation.[20] If we define the pair density matrix [Eq. (4)] as

$$\rho^0(\mathbf{R}_{i-1},\mathbf{R}_i,\tau)\exp[-U(\mathbf{R}_{i-1},\mathbf{R}_i,\tau)] \equiv \rho^0(\mathbf{R}_{i-1},\mathbf{R}_i,\tau)\exp(-U^i),$$

the virial estimator for the kinetic energy is given by

$$\mathcal{K}_V = \left\langle \frac{3N}{2M\tau} - \frac{1}{4M\tau^2\lambda}(\mathbf{R}_{M+i}-\mathbf{R}_i)(\mathbf{R}_{i+1}-\mathbf{R}_i) + \frac{1}{2\tau}\nabla_i(U^{i-1}+U^i)\Delta_i + \frac{dU^i}{d\tau} - V(\mathbf{R}_i) \right\rangle, \tag{5}$$

where $\lambda = \hbar^2/2m$ and $\Delta_i = \sum_{j=-M+1}^{M-1}(\mathbf{R}_i - \mathbf{R}_{i+j})$.

III. SYSTEM

We study ^{7}Li for a range of temperatures around melting. The system is modeled as a collection of lithium atoms interacting through an effective pair potential and confined in a box with periodic boundary conditions.

Although liquid lithium can be characterized, under suitable conditions, by a predominantly two-body central interaction, it should really be considered as a two-component mixture of interacting electrons and ions. It is, however, possible to regard lithium as a quasi-one-component liquid in which the ions move in an effective potential established by the electron gas.[18] The electron-ion interaction, described by a pseudopotential, is weak and can be considered as perturbing the electron gas treated as uniform to zeroth order. Within perturbation theory and linear response theory, it is possible to calculate the energy of the system of pseudoions and electrons for a given configuration of the ions. The energy acts as a potential energy for the ions alone and, to second-order perturbation theory, the effective interatomic potential is a pair potential.

If $v_{ps}(q)$ is the Fourier transform of the local electron-ion pseudopotential, the resulting effective pair interaction between the ions, $V(r)$, is the Fourier transform of $V(q)$:

$$V(q) = -\frac{4\pi Z_v^2}{q^2}\left\{1 + \left(\frac{1}{\epsilon(q)} - 1\right)\left[\frac{q^2}{4\pi Z_v} v_{ps}(q)\right]^2\right\}, \tag{6}$$

where Z_v is the valence charge of the pseudoion and $\epsilon(q)$ the dielectric function. Although a nonlocal pseudopotential could be employed, in the present work, we restrict ourselves to local pseudopotentials.

We consider the simple Ashcroft empty-core pseudopotential:[21]

$$v_{ps}(r) = \begin{cases} 0 & (r < R_c) \\ -Z_v/r & (r \geq R_c), \end{cases} \tag{7}$$

whose Fourier transform is given by

$$v_{ps}(q) = -\frac{4\pi Z_v}{q^2}\cos(qR_c). \tag{8}$$

We used $Z_v = 1$ and $R_c = 1.44$ a.u., which was fitted in Ref. 14 to reproduce the height of the main peak of the experimental structure factor.

To completely specify the form of the effective interatomic potential, we need to choose the local field factor $G(q)$ entering in the dielectric function $\epsilon(q)$:

$$\epsilon(q) = 1 - (4\pi/q^2)\chi_0(q)/[1 + (4\pi/q^2)G(q)\chi_0(q)], \tag{9}$$

where $\chi_0(q)$ is the Lindhard response function. A comparison of several approximate $G(q)$ with an accurate local field

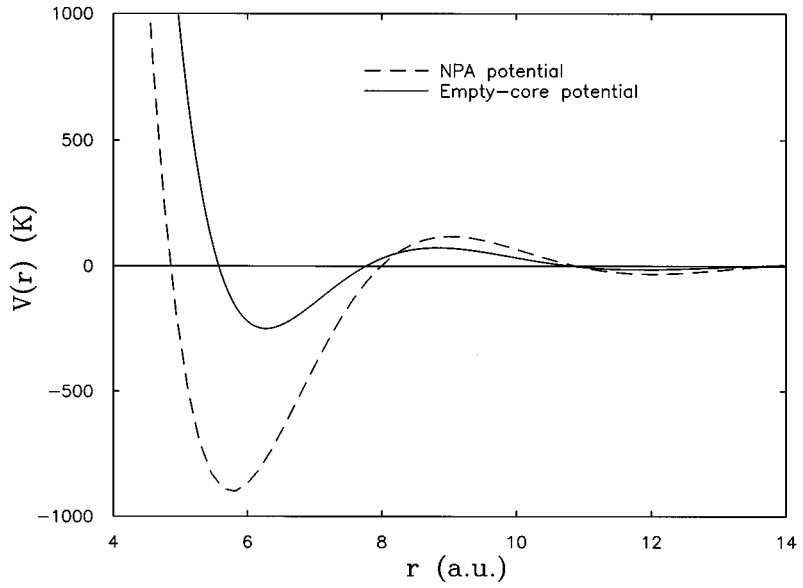

FIG. 1. Effective interatomic potentials for ^{7}Li at $T=470$ K and number density $\rho=0.5134$ g/cm^3. The full curve is obtained from the empty-core potential ($R_c=1.44$ a.u.) and the dashed curve from the NPA potential (Ref. 25).

factor determined by quantum Monte Carlo calculations is given in Ref. 22. The corresponding interatomic potentials constructed for sodium starting from an empty-core pseudopotential are shown in Ref. 23. The Ichimaru-Utsumi expression of the local field factor[24] yields a potential that, in the repulsive part, is quite close to the one obtained from the accurate $G(q)$. Since the predominant effect of the potential on the kinetic energy is given by its repulsive part,[7] we decided to adopt the Ichimaru-Utsumi expression for the local field factor. This choice also allows us to be consistent with classical molecular-dynamics simulations of liquid lithium already existing in the literature.[14]

The performance of the interatomic potential obtained from the empty-core pseudoion [Eqs. (6)–(8)] has been throughly tested within classical molecular dynamics. Structural and thermodynamic properties of liquid lithium are well reproduced by this potential.[13] Comparable results are obtained using potentials derived from the local neutral pseudoatom[13] (NPA) or a nonlocal pseudopotential.[11] On the other hand, recent x-ray high-resolution inelastic-scattering experiments[17] seem to indicate that the coherent dynamical structure factor is better reproduced by simulations using a potential derived from the NPA pseudoion.

In Fig. 1, we plot the lithium interatomic potential obtained from the empty-core and the NPA electron-ion potential[25] at a number density $\rho=0.5134$ g/cm^3 ($T=470$ K). Note that both potentials are density dependent, the empty-core potential through the dielectric function and the NPA potential through the electron-ion pseudopotential. Since the form of the two interatomic potentials is quite different (with a change of about 10% in the core radius), we evaluated the kinetic energy of the system using both potentials within PIMC.

IV. RESULTS AND CONCLUSIONS

We perform PIMC simulations of ^{7}Li in the solid and liquid phases between $T=300$ K and $T=520$ K. The temperatures and densities we considered are listed in Table I. For temperatures up to 450 K, we used the equilibrium densities of ^{7}Li at atmospheric pressure.[26] For temperatures above 470 K, the densities approximately correspond to the

TABLE I. Kinetic energy ($\mathcal{K}$) of ^{7}Li as a function of temperature for the empty-core pseudopotential. We list the excess kinetic energy and the percentage excess with respect to the classical kinetic energy, $\mathcal{K}_{\rm cl}=3/2k_{\rm B}T$. $\mathcal{K}_{\mathcal{O}(\hbar^2)}$ is the kinetic energy to second order in $\hbar$ [Eq. (10)]. The error on $\mathcal{K}_{\mathcal{O}(\hbar^2)}$ is estimated to be of the order of 0.5 K. The numbers in parentheses are the statistical errors on the last digit.

T (K)	Density (g/cm^3)	$\mathcal{K}$ (K)	$\mathcal{K}-\mathcal{K}_{\rm cl}$ (K)	$\mathcal{K}_{\mathcal{O}(\hbar^2)}-\mathcal{K}_{\rm cl}$ (K)	$(\mathcal{K}-\mathcal{K}_{\rm cl})/\mathcal{K}_{\rm cl}$ (%)
300	0.5387	496.83(6)	46.83(6)	45.4	10.41(1)
350	0.5348	562.99(7)	37.99(7)	38.6	7.24(1)
400	0.5308	632.96(4)	32.96(4)	33.4	5.49(1)
450	0.5261	705.03(5)	30.03(5)	29.2	4.45(1)
470	0.5134	732.66(8)	27.66(8)	27.2	3.92(1)
480	0.5126	747.11(6)	27.11(6)	26.6	3.77(1)
500	0.5110	775.90(5)	25.90(5)	25.4	3.45(1)
520	0.5093	804.85(6)	24.85(6)	24.3	3.19(1)

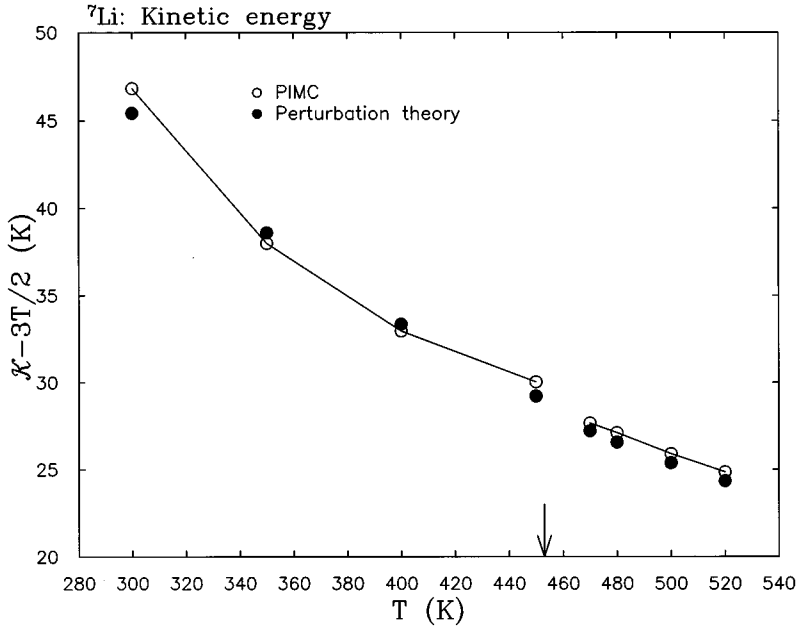

FIG. 2. Excess kinetic energy for ^{7}Li as a function of temperature. PIMC results are compared with the values obtained from Eq. (10). The calculations are performed using the potential derived from the empty-core pseudoion. The arrow indicates the experimental melting temperature $T_m = 453$ K.

equilibrium values for natural lithium.[27] The experimental melting temperature of ^{7}Li at atmospheric pressure is $T_m = 453$ K.

Above melting, we use 150 particles in a cubic box with periodic boundary conditions. In the solid phase, we arrange 250 particles in a bcc lattice and allow them to equilibrate. We are therefore neglecting the effect of vacancies or other defects in the solid phase near melting. By inspecting the pair-distribution function, we verified that the system was liquid for temperatures above T_m. We used the pair density matrix of Eq. (4) and the number M of slices [Eq. (2)] was set equal to 10. Convergence with respect to number of slices and number of particles was checked. The extrapolated kinetic energy for an infinite number of slices is half of a degree Kelvin smaller than the value obtained with ten time slices.

The interatomic potential was described in the previous section. As already mentioned, we also tested the dependence of the results on the form of the interatomic potential. At $T = 470$ K, we calculated the kinetic energy within PIMC using the potentials derived from the empty-core and the NPA pseudoion. The kinetic energy is given, respectively, by $\mathcal{K}_{\text{empty-core}} = (732.66 \pm 0.08)$ K and $\mathcal{K}_{\text{NPA}} = (730.72 \pm 0.08)$ K. Despite the large difference between the two potentials (Fig. 1), there is little change in the kinetic energy. As expected, the smaller core of the NPA potential yields a lower excess kinetic energy.

In Table I, we list the kinetic energy obtained by PIMC calculations as a function of temperature using the empty-core potential. The excess of kinetic energy decreases from 10.41(1)% at $T = 300$ K to 3.19(1)% at $T = 520$ K. Remarkably, the kinetic energy still differs from its classical value at temperature as high as 520 K confirming that the excess kinetic energy is a slowly decaying function of temperature.[8]

Since the quantum effects are not too large, an expansion of the kinetic energy in powers of $\hbar$ should be rapidly convergent. It is indeed possible to account for the leading quantum mechanical effects (exchange effects being exponentially small) through an expansion of the partition function Z in powers of $\hbar$.[19] The kinetic energy is obtained as $\mathcal{K} = -m\,\partial Z/\partial m$ and, to second order in $\hbar$, is given by

$$\mathcal{K} = \frac{3}{2}k_B T + \frac{\pi}{3}\frac{\hbar^2}{2m}\frac{1}{k_B T}\rho\int_0^\infty r^2 g(r)\left[\frac{d^2V(r)}{dr^2} + \frac{2}{r}\frac{dV(r)}{dr}\right]dr, \tag{10}$$

where $g(r)$ is the pair distribution function in the classical canonical ensemble. We use the pair distribution function obtained in our PIMC calculations to evaluate the quantum correction of Eq. (10) for the temperatures and densities reported in Table I. The results are shown in Table I and plotted in Fig. 2 together with the kinetic energies obtained within PIMC.

The results are not significantly affected by the use of the PIMC pair distribution function instead of the classical one: in this temperature and density range, the distribution function of lithium differs only slightly from the one we obtained within PIMC for a system of particles at the same density and temperature but a 100 times heavier mass.

The perturbative results are very close to the PIMC values with a discrepancy smaller than 1 K for temperatures greater than 300 K. This good agreement is also found when using the NPA potential. However, for neon in the solid phase, the PIMC kinetic energies[2] were found to be significantly different from the values obtained from a perturbation to order $\hbar^6$ (Ref. 28) showing that the series has a slow convergence at low temperatures.

We did not attempt the rather complex evaluation of higher-order corrections but we followed Ref. 5 in obtaining a high-temperature expansion of the kinetic energy. Since, at

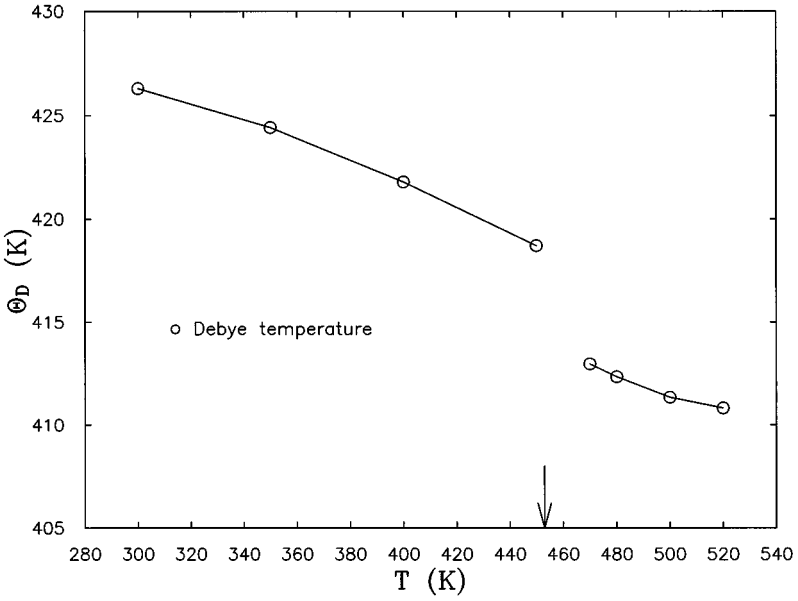

FIG. 3. Debye temperature defined to give the correct first quantum correction to the classical kinetic energy as in Eq. (10). The arrow indicates the experimental melting temperature $T_m = 453$ K.

the same density, the kinetic energies of the solid and the liquid are rather similar,[8] the liquid is also treated as a harmonic solid and the kinetic energy within the Debye model[29] is expanded in inverse temperature as

$$\mathcal{K} = \frac{3}{2}T\left[1 + \frac{1}{20}\left(\frac{\Theta_D}{T}\right)^2 - \frac{1}{1680}\left(\frac{\Theta_D}{T}\right)^4 + \frac{1}{151200}\left(\frac{\Theta_D}{T}\right)^6 + \cdots\right], \tag{11}$$

where, at each temperature and density, we define the Debye temperature as $\Theta_D^2 = (5\hbar^2/9M)\langle \Delta V(r)\rangle$ to yield the correct first quantum correction to the classical kinetic energy as in Eq. (10). As shown in Fig. 3, Θ_D varies only a few percent over the temperature range we considered. The kinetic energies from perturbation theory to order $\hbar^2$ [Eq. (10)] are not significantly affected by the additional terms in Eq. (11). However, the higher-order terms, while being of the correct order of magnitude, are not in quantitative agreement with the PIMC results.

Therefore, we can conclude that an expansion to second order in $\hbar$ is sufficient to account for the leading quantum corrections to the kinetic energy and other static properties and a classical treatment of lithium around the melting point is justified.

ACKNOWLEDGMENTS

This work was supported by the NSF (Grant No. DMR 9422496). C.F. thanks Erik Koch, Ralph Simmons, Massimo Boninsegni, and Giorgio Pastore for useful discussions. We are grateful to Massimo Boninsegni for a careful reading of the manuscript and to David González for providing the NPA potential. The calculations were performed on the IBM SP2 computer at the Cornell Theory Center.

[1] P. E. Sokol, T. R. Sosnick, and W. M. Snow, in *Momentum Distribution*, edited by R. Silver and P. E. Sokol (Plenum, New York, 1987).
[2] D. N. Timms, A. C. Evans, M. Boninsegni, D. M. Ceperley, J. Mayers, and R. O. Simmons, J. Phys.: Condens. Matter **8**, 6665 (1996).
[3] M. A. Fradkin, S.-X. Zeng, and R. O. Simmons, Z. Naturforsch. Teil A **48A**, 438 (1993).
[4] R. O. Simmons, Z. Naturforsch. Teil A **48A**, 415 (1993).
[5] R. T. Azuah, W. G. Stirling, H. R. Glyde, and M. Boninsegni, J. Low Temp. Phys. (to be published).
[6] A. C. Evans, J. Mayers, and D. N. Timms, Z. Naturforsch. Teil A **48A**, 425 (1993).
[7] M. Boninsegni, C. Pierleoni, and D. M. Ceperley, Phys. Rev. Lett. **72**, 1854 (1994).
[8] D. M. Ceperley, R. O. Simmons, and R. C. Blasdell, Phys. Rev. Lett. **77**, 115 (1996).
[9] A. C. Evans, J. Myers, and D. N. Timms, J. Phys.: Condens. Matter **6**, 4197 (1994).
[10] S. van der Aart, P. Verkerk, and J. Myers (private communications).
[11] W. Jank and J. Hafner, J. Phys.: Condens. Matter **2**, 5065 (1990).
[12] M. Canales, J. À. Padró, L. E. González, and A. Giró, J. Phys.: Condens. Matter **5**, 3095 (1993).
[13] L. E. González, D. J. González, M. Silbert, and J. A. Alonso, J. Phys.: Condens. Matter **5**, 4283 (1993).
[14] M. Canales, L. E. González, and J. À. Padró, Phys. Rev. E **50**, 3656 (1994).
[15] A. Torcini, U. Balucani, P. H. K. de Jong, and P. Verkerk, Phys. Rev. E **51**, 3126 (1995).
[16] P. H. K. de Jong, P. Verkerk, and L. A. de Graaf, J. Phys.: Condens. Matter **6**, 8391 (1994).
[17] H. Sinn, F. Sette, U. Bergmann, Ch. Halcoussis, M. Krisch, R.

Verbeni, and E. Burkel, Phys. Rev. Lett. **78**, 1715 (1997).
[18] N. W. Aschcroft and D. Stroud, in *Solid State Physics*, edited by H. Ehrenreich, F. Seitz, and D. Turnbull (Academic, New York, 1978).
[19] E. Wigner, Phys. Rev. **40**, 749 (1932); J. G. Kirkwood, *ibid.* **44**, 31 (1933).
[20] D. M. Ceperley, Rev. Mod. Phys. **67**, 279 (1995).
[21] N. W. Ashcroft, Phys. Lett. **23**, 48 (1966).
[22] S. Moroni, D. M. Ceperley, and G. Senatore, Phys. Rev. Lett. **75**, 689 (1995).
[23] G. Senatore, S. Moroni, and D. M. Ceperley, J. Non-Cryst. Solids **207**, 851 (1996).
[24] S. Ichimaru and K. Utsumi, Phys. Rev. B **24**, 7385 (1981).
[25] D. J. Gonzalez (private communications).
[26] T. N. Mel'nikova and A. G. Mozgovoi, High Temp. **26**, 6848 (1988).
[27] *Handbook of Thermodynamic and Transport Properties of Alkali Metals*, edited by R. W. Ohse (Blackwell Scientific Publications, Oxford, 1985).
[28] M. Asger and Q. N. Usmani, Phys. Rev. B **49**, 12 262 (1994).
[29] A. A. Maradudin, E. W. Montroll, G. W. Weiss, and I. P. Ipatova, *Theory of Lattice Dynamics in the Harmonic Approximation*, Solid State Supplement **3** (Academic Press, New York, 1963).